This is a repository copy of *Vertical field inhomogeneity associated with threading dislocations in GaN high electron mobility transistor epitaxial stacks*.

White Rose Research Online URL for this paper:
https://eprints.whiterose.ac.uk/183916/

Version: Accepted Version

Article:

Wohlfahrt, M., Uren, M.J., Yin, Y. et al. (2 more authors) (2021) Vertical field inhomogeneity associated with threading dislocations in GaN high electron mobility transistor epitaxial stacks. Applied Physics Letters, 119 (24). 243502. ISSN 0003-6951

https://doi.org/10.1063/5.0066346

This article may be downloaded for personal use only. Any other use requires prior permission of the author and AIP Publishing. This article appeared in Markus Wohlfahrt, Michael J. Uren, Yidi Yin, Kean Boon Lee, and Martin Kuball , "Vertical field inhomogeneity associated with threading dislocations in GaN high electron mobility transistor epitaxial stacks", Appl. Phys. Lett. 119, 243502 (2021) https://doi.org/10.1063/5.0066346 and may be found at https://aip.scitation.org/doi/full/10.1063/5.0066346.

Reuse

Items deposited in White Rose Research Online are protected by copyright, with all rights reserved unless indicated otherwise. They may be downloaded and/or printed for private study, or other acts as permitted by national copyright laws. The publisher or other rights holders may allow further reproduction and re-use of the full text version. This is indicated by the licence information on the White Rose Research Online record for the item.

Takedown

If you consider content in White Rose Research Online to be in breach of UK law, please notify us by emailing eprints@whiterose.ac.uk including the URL of the record and the reason for the withdrawal request.

eprints@whiterose.ac.uk
https://eprints.whiterose.ac.uk/

Vertical field inhomogeneity associated with threading dislocations in GaN High Electron Mobility Transistor epitaxial stacks

Markus Wohlfahrt[1*], Michael J. Uren[1], Yidi Yin[2], Kean-Boon Lee[2], Martin Kuball[1]

[1]*Centre for Device Thermography and Reliability (CDTR), H.H. Wills Physics Laboratory, University of Bristol, Bristol, BS8 1TL, UK*

[2]*Department of Electronic and Electrical Engineering, University of Sheffield, Sheffield, S1 3JD, UK*

*markus.wohlfahrt@bristol.ac.uk (corresponding author)

A measurement technique combining Kelvin-Probe Force Microscopy (KPFM) with substrate bias is developed and demonstrated on AlGaN/GaN-on-Si device structures, under conditions relevant to the effect of off-state drain bias stress in transistors. For high substrate bias, the measurements show a significantly lowered surface potential surrounding a small proportion of the dislocations imaged with atomic force microscopy (AFM), laterally extending on a scale of up to a micrometer. Both the density and the size of those features increase with substrate bias, however, conductive AFM measurements under the same bias conditions showed no leakage reaching the surface associated with those features. Our model considers localized conductive paths that end a certain distance below the 2DEG electrically "thinning" the epitaxy and therefore deforming the potential and increasing electric field under off-state stress bias. The conclusion is that the vertical electric field in the buffer is laterally highly non-uniform, with an enhanced vertical field in the vicinity of those dislocations. This non-uniformity redirects substrate bias stress from the buffer to the channel with potential consequences for breakdown.

With its excellent material properties, Gallium Nitride (GaN) is highly suitable for power switching and radio frequency amplifying applications[1]. The AlGaN/GaN High Electron Mobility Transistor (HEMT) already achieved significant commercialization owing to the high electron mobility as well as high breakdown field[2]. However, devices are still subject to inherent problems like reversible and irreversible degradation processes, particularly when grown on Si[3, 4]. Point defects or extended defect paths such as threading dislocations allow charge carrier trapping and leakage currents[5, 6]. Both are known to have a crucial impact on device reliability and performance[7]. Large efforts have been spent on reducing the dislocation density to decrease vertical leakage in the devices[8]. Dislocation density for AlGaN/GaN grown on Si is typically around 10^9 cm^{-2} [9-13], of which the screw and mixed type (screw + edge) dislocations are known to act as leakage paths in Schottky diodes under high voltage reverse bias conditions[14-16]. Reported densities of conductive dislocations, often correlated to device breakdown behavior, are in the range 3 - 4 × 10^7 cm^{-2} [6, 12, 17-19]. However, correlating device leakage characteristics and breakdown values to the density of dislocations is not that straightforward as bulk leakage also depends on other parameters such as carbon (C) doping. Measuring the density of conductive dislocations, typically by conductive AFM, is often flawed as a leakage spot at the surface does not necessarily mean an underlying vertically conductive dislocation through the entire buffer due to shunting effects of the 2DEG[20]. It is also not understood how a single, potentially partially conductive dislocation with certain current-voltage (IV) characteristics contributes to overall device breakdown[21]. Therefore, neither measuring buffer leakage nor investigating dislocation density or conductivity of different types is sufficient to characterize and model device breakdown. On the other hand, leakage along threading dislocations is also known to facilitate efficient discharging of the buffer following trapping under stressed conditions, particularly when C-doped buffer layers are involved. This hugely benefits dynamic device performance following switching from off-state to on-state[22-25]. This ultimately leads to a tradeoff between a low density of conductive dislocations to ensure low high field leakage impacting breakdown, and sufficient dislocation-originated leakage to achieve good dynamic device performance[26]. Therefore, a good understanding of dislocations as well as the associated electrical properties and leakage currents is important for device reliability.

In this work, we introduce a measurement technique which demonstrates that leaky threading dislocations induce large potential deformations during off-state substrate bias, and by extension drain bias. During substrate bias stress, this shows an apparent depletion region in the 2D electron gas (2DEG) surrounding dislocations and extending up to a micrometer scale. The approach combines two methodologies: Kelvin-Probe Force Microscopy (KPFM) and substrate bias. KPFM is a surface-sensitive technique that allows the mapping of the surface potential represented as contact potential difference (CPD) with respect to the probe work function[27]. Substrate bias probes electrical buffer characteristics and yields information about vertical leakage and charge storage mechanisms in AlGaN/GaN HEMTs[23]. Combining both techniques allows imaging of the impact of the whole buffer leakage path on the 2DEG under close-to-operating conditions with sub-micrometer lateral resolution.

The sample studied was grown using MOCVD and consists of about 2.5 μm graded (Al,Ga)N buffer on a Si substrate followed by 500 nm C doped GaN, an unintentionally doped 250 nm thick GaN channel, a 25 nm thick AlGaN barrier with 25% Al composition as well as a 2 nm GaN cap. The sample was processed with Ti/Al/Ni/Au ohmic contacts alloyed at 800 °C in nitrogen ambient with Ti/Au top metal layer using circular Transfer Length Method (TLM) structures with a shared outer ohmic contact, as shown in the inset of Fig. 1. The TLM gap spacing used here was 25 μm. The channel resistance was 600 **Ω**/sq. The circular TLMs allow measurement of the 2DEG conductivity as a function of negative Si substrate (back-gate) bias, while the absence of passivation allows simultaneous access to the GaN cap surface. This allows KPFM in the TLM gap, as well as visualization of atomic steps and surface dislocation pits using AFM as can be seen in Fig. 2. The area of the outer ohmic contact, electrically grounded, was deliberately as large as possible, extending to 5 mm × 5 mm to reduce KPFM noise by maximally shielding the KPFM detection system (sitting above the sample and operating in the millivolt range) from large substrate biases of hundreds of volts. The grounded source contact and therefore grounded 2DEG also reproduces the vertical field magnitude and sign used during substrate voltage ramps and regular positive drain bias operating conditions.

FIG. 1. Substrate ramp of the investigated sample with a shared downward sweep and return sweeps from different maximum voltages. The inset shows the test structure used. It is a set of circular TLMs with shared outer ohmic contact and varying gap spacing to the inner 100 μm diameter ohmic contact. There are three circular TLMs each for gap spacing of 10 (top), 15, 20, and 25 μm (bottom). This TLM assembly sits embedded in a large 5 mm × 5 mm outer ohmic contact to shield the AFM probe from substrate fields.

Scanning probe was used in the dual-pass (lift mode) amplitude-modulated (AM) KPFM mode paired with tapping mode[28-30]. In this study, the lift height for the reverse trace was 20 nm. Conductive AFM was measured with a substrate voltage up to -200V using highly doped diamond probes (Nanosensors CDT-NCHR) while keeping the probe grounded. In substrate ramps, the channel conductivity was monitored by applying a small bias (typically 1 V) between two ohmic contacts on the top of the AlGaN/GaN-on-Si stack while a bidirectional negative substrate voltage sweep was applied to the Si (Fig. 1). The channel conductivity is related to the 2DEG concentration which acts as a sensor of the electric field directly below the 2DEG. Depending on the maximum sweep voltage and resulting current hysteresis loop, different buffer transport mechanisms are probed. Capacitive coupling happens if the buffer behaves as an insulator and the leakage in the entire buffer is smaller than the displacement current. Depending on which layer starts to conduct, charge can either be redistributed within that layer to form a dipole, or alternatively charge can flow from the contacts, with either case leading to charge accumulation in depletion regions or at blocking interfaces[23]. This charging causes a deviation from pure capacitive behavior and its linear relationship. Fig. 1 shows a fairly normal substrate ramp characteristic for a good quality epitaxy, with positive charge storage when sweeping to -100 V that gets neutralized on the return sweep when approaching 0 V. When sweeping to −300 V, a deviation occurs in the opposite direction representing small negative charge storage which is still present when the bias is removed[31].

FIG. 2. AFM topography scan of GaN surface. The marked dislocations are spots that are analyzed in terms of surface potential in Fig. 3.

Fig. 3a shows a sequence from CPD measurements taken in -25 V substrate bias steps down to -200 V. After each voltage step, the sample was allowed 2 min to stabilize at the new bias conditions before measuring the CPD. At substrate biases down to -100 V, the surface potential was uniform with no apparent features. Past this voltage, spots appeared with lower surface potential becoming more pronounced and increasing in size, with further spots appearing the more negative the voltage. Approaching a substrate voltage of -200 V, two-thirds of the pinch-off voltage (Fig. 1), the size of the spots reached up to 1 μm in diameter. At a substrate voltage of -200 V, the signal-to-noise ratio for the CDP signal increased. The maximum sweep voltage was also limited by the presence of a large series resistor (33 M**Ω**) in the bias line, required to prevent damage to the KPFM instrument in the event of sample breakdown. Beyond -200 V the increase in substrate leakage started to result in a significant voltage drop across the series resistor. Stepping the substrate bias back towards 0 V, the trend was reversed with some latency. The features gradually disappeared, however, a center spot as a superposition of several CDP features remained weakly present at 0 V (Fig. 3a). In Fig. 3b, the CPD is plotted at the three marked spots in Figs. 2 and 3a. The potential is referenced to a location far away from any dislocation feature to account for potential drift associated with fringing fields coupling the substrate voltage to the AFM head. The surface potential is initially substrate bias independent, but above a specific substrate bias (-100 V), the surface potential starts to decrease rapidly.

FIG. 3. a) Selection of contact potential difference (CPD) images with decreasing substrate voltage to -200 V and the return to no substrate bias in increments of 25 V from top left to bottom right (quadruple scale at -200 V). The reference spot is chosen far away from apparent dislocation features. b) Quantitative analysis of spots 1, 2, and 3 relative to the respective reference values for the downward and return sweep of substrate voltage. CPD values for the analyzed spots were averaged over a diameter of 200 nm. The inset shows a schematic of the conductive AFM measurement with different types of leakage paths (a: substrate to surface, b: substrate to 2DEG, c: substrate to buffer).

All CPD spots appearing for high negative substrate voltages can clearly be correlated to the location of a screw dislocation in the topography image (Fig. 2). Threading edge dislocations typically form small depressions whereas threading screw dislocations lead to larger depressions[9]. The density of the observed features in Fig. 3a showing a significantly lower surface potential is ~4 × 10^7 cm^{-2} which is consistent with reported densities of 3 - 4 × 10^7 cm^{-2} for conductive dislocations[6, 12, 17-21]. Interestingly, measuring conductive AFM under the same conditions as the CDP measurements with a grounded 2DEG, a grounded AFM probe, the large series safety resistor (33 M**Ω**) present, and a bias applied to the substrate does not reveal any leakage paths reaching the surface. This was the case for measurements covering the entire substrate voltage range to the pinch-off voltage of -300 V with high contact force using high spring constant AFM probes to ensure good electrical contact between probe and sample. The conductive AFM result was somewhat unexpected since previous reports of conductive AFM using lower biases on GaN epitaxy revealed local leakage spots reaching the surface[6, 12, 17-21]. However, those studies were conducted with a floating 2DEG, hence allowing the full applied voltage to be dropped across the top barrier layer. The conductive AFM measurement reported here suggests that the presence of the grounded 2DEG clamps the dislocation potential and connects any electrically conductive dislocations in the buffer to ground, similar to the suggestion in some previous reports[17, 21]. Fig. 3b inset schematically shows the possible leakage paths. The latency between down-sweep and return-sweep observed in Fig. 3b indicates a charging effect associated with the screw dislocation. This effect may represent a previously unreported localized mechanism for dynamic R_{ON}.

FIG. 4. Schematic of the electrostatics around a conductive path as opposed to a pristine buffer with KPFM measurement on the surface and higher electric field in the gap between conductive dislocation and 2DEG.

The observed change in CPD in the 2DEG can be explained using a model that considers the electrostatics as illustrated schematically in Fig. 4. Far away from the dislocation, the potential is dropped linearly and vertically between 2DEG and substrate along R_{Buffer} establishing an electric field E_{Buffer} (assuming no charge trapping or accumulation). However, with a conductive path along the dislocation core to the 2DEG, the distribution of potential is strongly dependent on the specific conductive properties of the dislocation. A lower resistivity along the dislocation ($R_{Conductive\ path} < R_{Buffer}$) extending partway through the epitaxy leads to a more negative potential at the top of the dislocation compared to the surrounding buffer. The conductive path has effectively electrically "thinned" the epitaxy at the location of the dislocation. This leads to a more concentrated electric field ($E_{Above\ conductive\ path} > E_{Buffer}$) from the top of the dislocation across the gap (R_{Gap}) to the 2DEG causing a localized depletion in the 2DEG ($R_{Depletion}$) region. This results in a reduced potential at the surface across the barrier ($R_{Barrier}$) at the location of the dislocation ($V_{Above\ conductive\ path} < V_{Above\ buffer}$) as observed in the KPFM measurements. It can be expected that this effect persists even when the conductive path ends deep in the buffer for a sufficiently conductive dislocation. Furthermore, the magnitude of the effect is directly proportional to the conductivity of the path ($\propto {R_{Conductive\ path}}^{-1}$) and inversely proportional to the depth where the conductive path ends underneath the 2DEG ($\propto d^{-1}$). It is known that the conductivity of dislocations can be modified by processing[32]. It has also been shown that processing can change the conductivity partway through the epitaxy, although in that case, it was an increase in conductivity in the upper part of the stack[33]. The mechanism is speculative but may be associated with decoration (or the removal of decoration) of the dislocation core with contaminants such as hydrogen during processing. While the proposed model explains the observed data, further validation including the consideration of alternative explanations is required to show the origin of the effect.

The observed potential deformation at off-state stress has implications for breakdown and vertical leakage. The higher the lower part dislocation conductivity, the greater is the electric field below the 2DEG in the vicinity of the dislocation. The measurements suggest that breakdown can be a highly localized phenomenon driven by a non-uniform potential distribution through the epitaxy. This becomes apparent from the large local depletion in the 2DEG, indicated by micrometer size surface potential features (Fig. 3a). This increases the electric field in the top GaN buffer layers, especially the channel, relative to the bulk of the buffer. Instead of dropping the voltage uniformly across the buffer, the channel gets locally exposed to a higher level of electric field stress. Hence, breakdown and vertical leakage could not simply be modeled as a bulk effect of the buffer stack but may well be driven by a small number of relatively conductive dislocations. Our measurement particularly suggests that threading dislocations that are not fully conductive from buffer to the surface (spots in fig. 3a) still cause significant potential deformations at off-state stress. This type of dislocation and its breakdown contribution has not been directly observed before and has only been inferred from indirect capacitance measurements[33]. Therefore, dislocation-induced breakdown ~~is~~ may well be more complicated than only considering apparent and conventionally measurable conductive dislocations.

In conclusion, we clearly demonstrated the complexity of dislocation-induced breakdown. Our substrate-biased KPFM measurements reveal inhomogeneities of the 2DEG at negative substrate voltages which relate to high off-state device stress. The more negative the substrate voltage, the more local 2DEG-depleted areas occur, marked by surface potential features, reaching up to 1 μm in diameter. This effect is consistent with a significant potential deformation and a highly non-uniform electric field distribution through the epitaxy stressing the channel instead of the buffer. It suggests that breakdown is not a bulk effect but can be highly localized. We particularly propose that the measurement can be explained by the conductive portion of a threading dislocation extending only partway through the epitaxial stack.

Bristol acknowledges partial financial support from the UK Engineering and Physical Sciences Research Council (RCUK) under EP/N031563/1. MK's position was supported by the Royal Academy of Engineering under the Chairs in Emerging Technologies scheme. MW acknowledges helpful discussions with Sven Besendörfer. KBL acknowledges financial support from the UK Engineering and Physical Sciences Research Council (RCUK) under EP/N015878/1.

Data availability statement:
The data that support the findings of this study are available from the corresponding author upon reasonable request.

[1]H. Amano, Y. Baines, E. Beam, et al., *The 2018 GaN power electronics roadmap*, Journal of Physics D: Applied Physics. **51**, (2018).

[2]K. Husna Hamza and D. Nirmal, *A review of GaN HEMT broadband power amplifiers*, AEU - International Journal of Electronics and Communications. **116**, 153040 (2020).

[3]G. Meneghesso, M. Meneghini, I. Rossetto, D. Bisi, S. Stoffels, M. Van Hove, S. Decoutere and E. Zanoni, *Reliability and parasitic issues in GaN-based power HEMTs: a review*, Semiconductor Science and Technology. **31**, (2016).

[4]J.A. del Alamo and J. Joh, *GaN HEMT reliability*, Microelectronics Reliability. **49**, 1200-1206 (2009).

[5]M. Meneghini, A. Tajalli, P. Moens, A. Banerjee, E. Zanoni and G. Meneghesso, *Trapping phenomena and degradation mechanisms in GaN-based power HEMTs*, Materials Science in Semiconductor Processing. **78**, 118-126 (2018).

[6]B. Kim, D. Moon, K. Joo, S. Oh, Y.K. Lee, Y. Park, Y. Nanishi and E. Yoon, *Investigation of leakage current paths in n-GaN by conductive atomic force microscopy*, Applied Physics Letters. **104**, (2014).

[7]M. Knetzger, E. Meissner, J. Derluyn, M. Germain and J. Friedrich, *Correlation of carbon doping variations with the vertical breakdown of GaN-on-Si for power electronics*, Microelectronics Reliability. **66**, 16-21 (2016).

[8]A. Lesnik, M.P. Hoffmann, A. Fariza, J. Bläsing, H. Witte, P. Veit, F. Hörich, C. Berger, J. Hennig, A. Dadgar and A. Strittmatter, *Properties of C-doped GaN*, physica status solidi (b). **254**, (2017).

[9]B. Heying, E.J. Tarsa, C.R. Elsass, P. Fini, S.P. DenBaars and J.S. Speck, *Dislocation mediated surface morphology of GaN*, Journal of Applied Physics. **85**, 6470-6476 (1999).

[10] T. Hino, S. Tomiya, T. Miyajima, K. Yanashima, S. Hashimoto and M. Ikeda, *Characterization of threading dislocations in GaN epitaxial layers*, Applied Physics Letters. **76**, 3421-3423 (2000).

[11] P. Visconti, K.M. Jones, M.A. Reshchikov, R. Cingolani, H. Morkoç and R.J. Molnar, *Dislocation density in GaN determined by photoelectrochemical and hot-wet etching*, Applied Physics Letters. **77**, 3532-3534 (2000).

[12] B.S. Simpkins, E.T. Yu, P. Waltereit and J.S. Speck, *Correlated scanning Kelvin probe and conductive atomic force microscopy studies of dislocations in gallium nitride*, Journal of Applied Physics. **94**, 1448-1453 (2003).

[13] A. Krtschil, A. Dadgar and A. Krost, *Decoration effects as origin of dislocation-related charges in gallium nitride layers investigated by scanning surface potential microscopy*, Applied Physics Letters. **82**, 2263-2265 (2003).

[14] M. Moseley, A. Allerman, M. Crawford, J.J. Wierer, M. Smith and L. Biedermann, *Electrical current leakage and open-core threading dislocations in AlGaN-based deep ultraviolet light-emitting diodes*, Journal of Applied Physics. **116**, (2014).

[15] S. Usami, Y. Ando, A. Tanaka, K. Nagamatsu, M. Deki, M. Kushimoto, S. Nitta, Y. Honda, H. Amano, Y. Sugawara, Y.-Z. Yao and Y. Ishikawa, *Correlation between dislocations and leakage current of p-n diodes on a free-standing GaN substrate*, Applied Physics Letters. **112**, (2018).

[16] J.W.P. Hsu, M.J. Manfra, D.V. Lang, S. Richter, S.N.G. Chu, A.M. Sergent, R.N. Kleiman, L.N. Pfeiffer and R.J. Molnar, *Inhomogeneous spatial distribution of reverse bias leakage in GaN Schottky diodes*, Applied Physics Letters. **78**, 1685-1687 (2001).

[17] S. Besendörfer, E. Meissner, A. Lesnik, J. Friedrich, A. Dadgar and T. Erlbacher, *Methodology for the investigation of threading dislocations as a source of vertical leakage in AlGaN/GaN-HEMT heterostructures for power devices*, Journal of Applied Physics. **125**, (2019).

[18] J.W.P. Hsu, M.J. Manfra, R.J. Molnar, B. Heying and J.S. Speck, *Direct imaging of reverse-bias leakage through pure screw dislocations in GaN films grown by molecular beam epitaxy on GaN templates*, Applied Physics Letters. **81**, 79-81 (2002).

[19] J.C. Moore, J.E. Ortiz, J. Xie, H. Morkoç and A.A. Baski, *Study of leakage defects on GaN films by conductive atomic force microscopy*, Journal of Physics: Conference Series. **61**, 90-94 (2007).

[20] S. Besendörfer, E. Meissner, T. Zweipfennig, H. Yacoub, D. Fahle, H. Behmenburg, H. Kalisch, A. Vescan, J. Friedrich and T. Erlbacher, *Interplay between C-doping, threading dislocations, breakdown, and leakage in GaN on Si HEMT structures*, AIP Advances. **10**, (2020).

[21] S. Besendorfer, E. Meissner, F. Medjdoub, J. Derluyn, J. Friedrich and T. Erlbacher, *The impact of dislocations on AlGaN/GaN Schottky diodes and on gate failure of high electron mobility transistors*, Sci Rep. **10**, 17252 (2020).

[22] M.J. Uren, M. Cäsar, M.A. Gajda and M. Kuball, *Buffer transport mechanisms in intentionally carbon doped GaN heterojunction field effect transistors*, Applied Physics Letters. **104**, 263505 (2014).

[23] M.J. Uren, S. Karboyan, I. Chatterjee, A. Pooth, P. Moens, A. Banerjee and M. Kuball, *"Leaky Dielectric" Model for the Suppression of Dynamic R_{ON} in Carbon-Doped AlGaN/GaN HEMTs*, IEEE Transactions on Electron Devices. **64**, 2826-2834 (2017).

[24] H. Yacoub, D. Fahle, M. Eickelkamp, A. Wille, C. Mauder, M. Heuken, H. Kalisch and A. Vescan, *Effect of stress voltage on the dynamic buffer response of GaN-on-silicon transistors*, Journal of Applied Physics. **119**, (2016).

[25] M.J. Uren and M. Kuball, *Impact of carbon in the buffer on power switching GaN-on-Si and RF GaN-on-SiC HEMTs*, Japanese Journal of Applied Physics. **60**, (2021).

[26] H. Yacoub, T. Zweipfennig, G. Lukens, H. Behmenburg, D. Fahle, M. Eickelkamp, M. Heuken, H. Kalisch and A. Vescan, *Effect of Carbon Doping Level on Static and Dynamic Properties of AlGaN/GaN Heterostructures Grown on Silicon*, IEEE Transactions on Electron Devices. **65**, 3192-3198 (2018).

[27] M. Nonnenmacher, M.P. O'Boyle and H.K. Wickramasinghe, *Kelvin probe force microscopy*, Applied Physics Letters. **58**, 2921-2923 (1991).

[28] V. Panchal, R. Pearce, R. Yakimova, A. Tzalenchuk and O. Kazakova, *Standardization of surface potential measurements of graphene domains*, Sci Rep. **3**, 2597 (2013).

[29] L. Collins, J.I. Kilpatrick, S.V. Kalinin and B.J. Rodriguez, *Towards nanoscale electrical measurements in liquid by advanced KPFM techniques: a review*, Rep Prog Phys. **81**, 086101 (2018).

[30] G. Stan, *High-speed digitization of the amplitude and frequency in open-loop sideband frequency-modulation Kelvin probe force microscopy*, Nanotechnology. **31**, 385706 (2020).

[31] F. Wach, M.J. Uren, B. Bakeroot, M. Zhao, S. Decoutere and M. Kuball, *Low Field Vertical Charge Transport in the Channel and Buffer Layers of GaN-on-Si High Electron Mobility Transistors*, IEEE Electron Device Letters. **41**, 1754-1757 (2020).

[32] W.M. Waller, M. Gajda, S. Pandey, J.J.T.M. Donkers, D. Calton, J. Croon, J. Sonsky, M.J. Uren and M. Kuball, *Control of Buffer-Induced Current Collapse in AlGaN/GaN HEMTs Using SiNx Deposition*, IEEE Transactions on Electron Devices. **64**, 4044-4049 (2017).

[33] B. Rackauskas, M.J. Uren, S. Stoffels, M. Zhao, B. Bakeroot, S. Decoutere and M. Kuball, *The Impact of Ti/Al Contacts on AlGaN/GaN HEMT Vertical Leakage and Breakdown*, IEEE Electron Device Letters. **39**, 1580-1583 (2018).

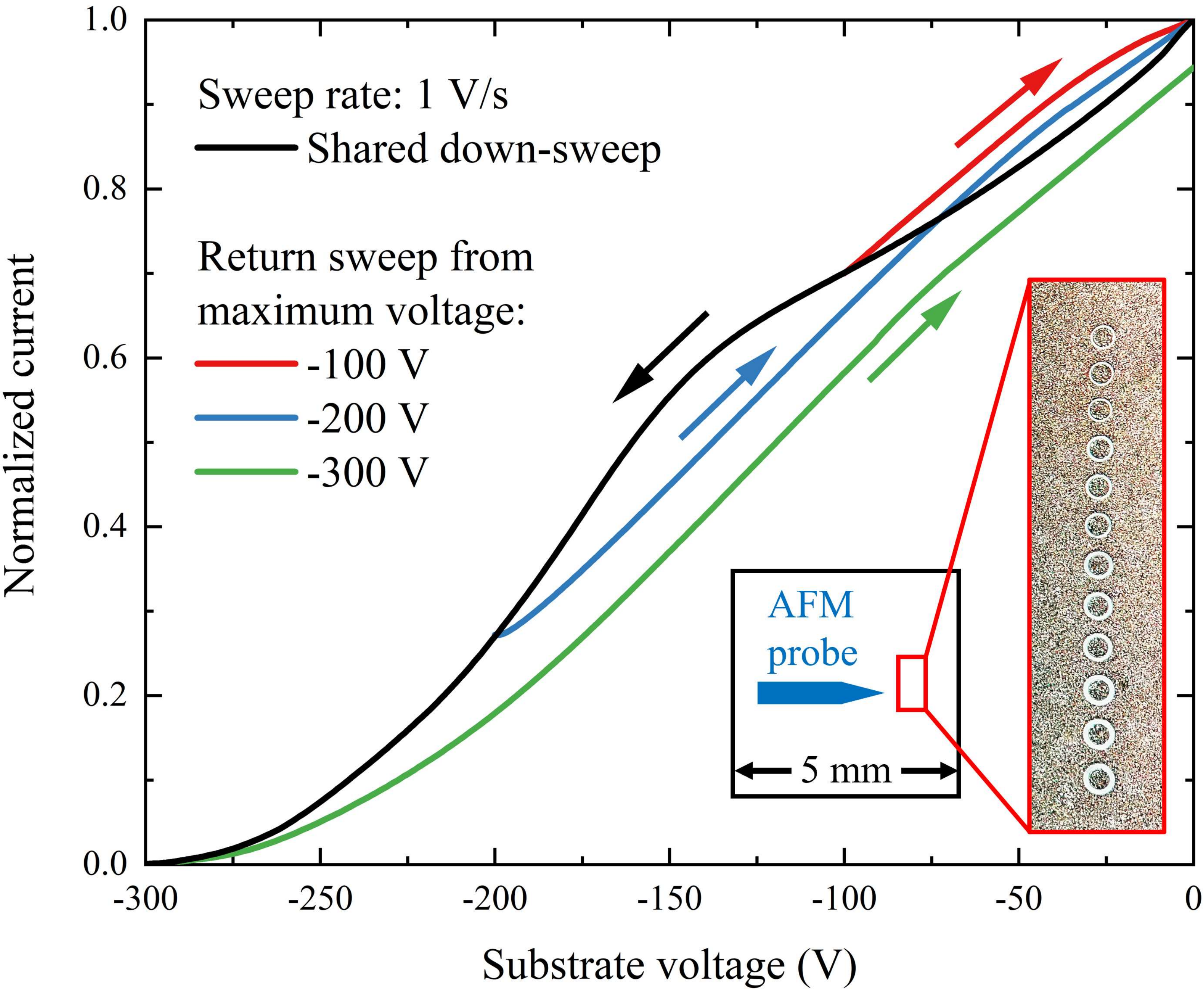
Sweep rate: 1 V/s
Shared down-sweep
Return sweep from maximum voltage:
-100 V
-200 V
-300 V
AFM probe
5 mm
Normalized current
0.0
0.2
0.4
0.6
0.8
1.0
Substrate voltage (V)
-300
-250
-200
-150
-100
-50
0

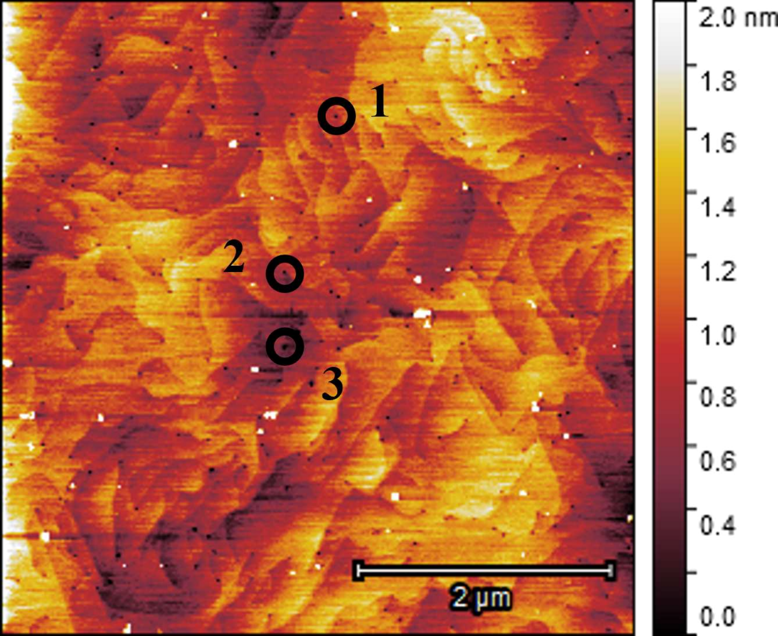
1
2
3
2 µm
2.0 nm
1.8
1.6
1.4
1.2
1.0
0.8
0.6
0.4
0.0

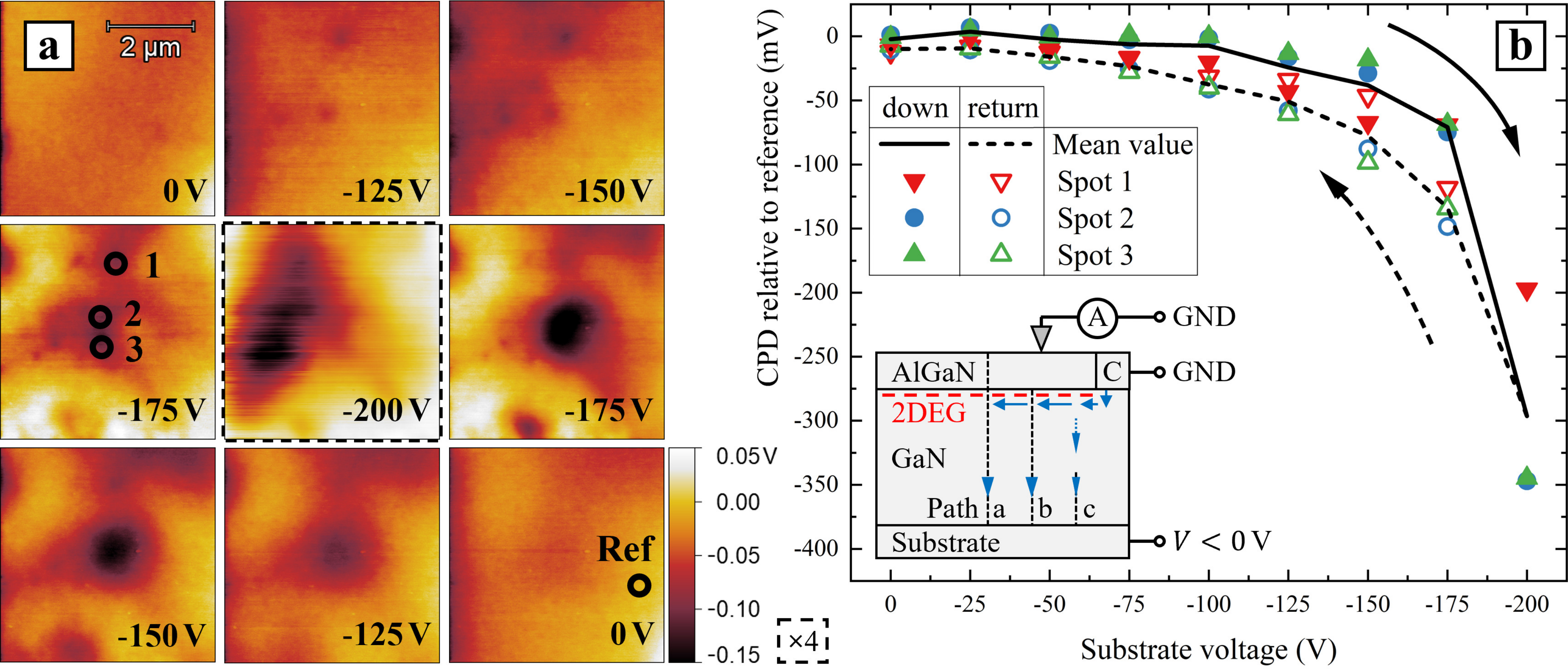
a
2 µm
0 V
-125 V
-150 V
1
2
3
-175 V
-200 V
-175 V
-150 V
-125 V
Ref
0 V
0.05 V
0.00
-0.05
-0.10
-0.15
×4
b
CPD relative to reference (mV)
Substrate voltage (V)
0
-50
-100
-150
-200
-250
-300
-350
-400
0
-25
-50
-75
-100
-125
-150
-175
-200
down
return
Mean value
Spot 1
Spot 2
Spot 3
A
GND
AlGaN
C
GND
2DEG
GaN
Path
a
b
c
Substrate
$V < 0$ V

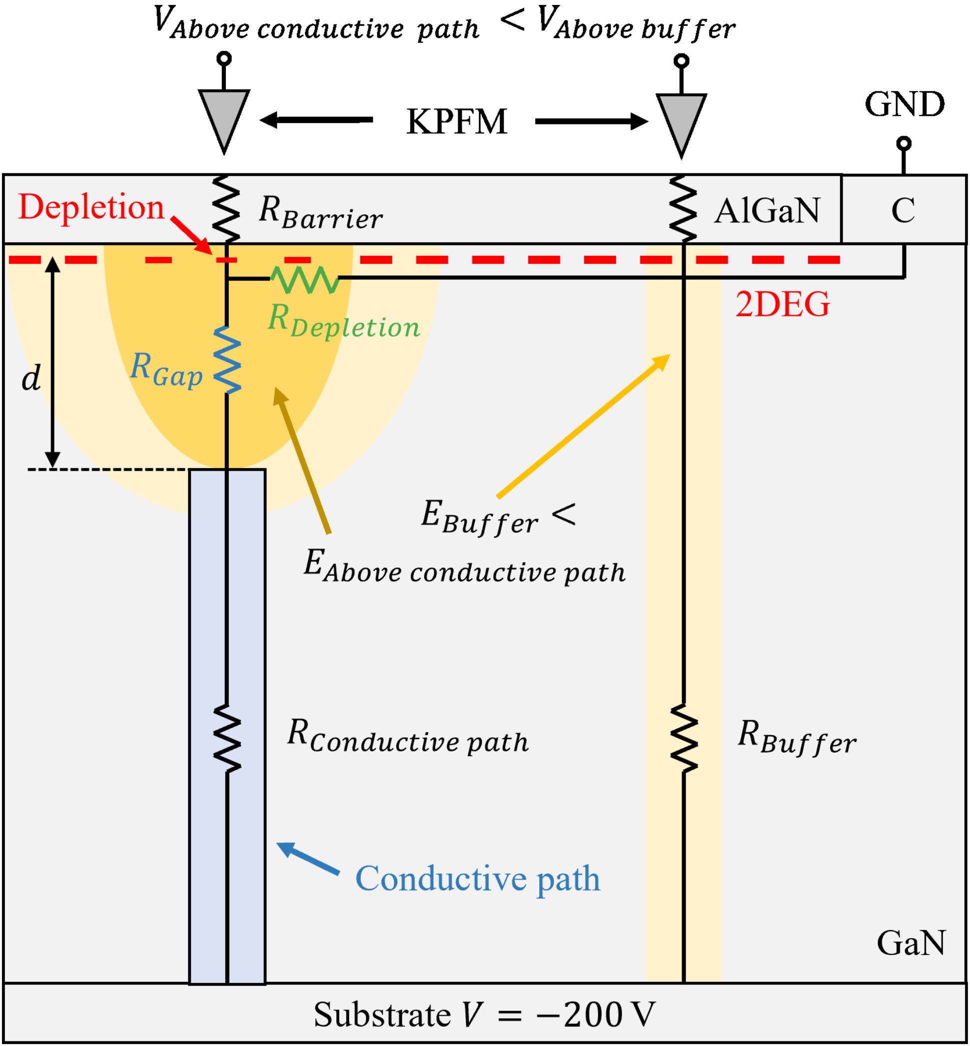
$V_{Above\ conductive\ path} < V_{Above\ buffer}$
KPFM
GND
Depletion
$R_{Barrier}$
AlGaN
C
2DEG
$R_{Depletion}$
R_{Gap}
d
$E_{Buffer} <$
$E_{Above\ conductive\ path}$
$R_{Conductive\ path}$
R_{Buffer}
Conductive path
GaN
Substrate $V = -200$ V